



Graphene Oxide-Modified Microcapsule Self-Healing System for 4D Printing

Bowen Ma¹, Yuping Zhang², Yongjie Wei¹, Mingrui Li¹ and Dongdong Li^{3*}

¹ Key Laboratory of Automobile Materials of Minister of Education, Department of Materials Science and Engineering, Jilin University, Changchun, China, ² School of Chemistry and Chemical Engineering, Huazhong University of Science and Technology, Wuhan, China, ³ State Key Laboratory for Materials Processing and Die and Mould Technology, School of Materials Science and Engineering, Huazhong University of Science and Technology, Wuhan, China

OPEN ACCESS

Edited by:

Kun Zhou,
Nanyang Technological University,
Singapore

Reviewed by:

Jiayao Chen,
Nanyang Technological University,
Singapore
Huijun Li,
Nanyang Technological University,
Singapore

*Correspondence:

Dongdong Li
lidongdong0@hust.edu.cn

Specialty section:

This article was submitted to
Smart Materials,
a section of the journal
Frontiers in Materials

Received: 24 January 2021

Accepted: 18 March 2021

Published: 16 April 2021

Citation:

Ma B, Zhang Y, Wei Y, Li M and
Li D (2021) Graphene Oxide-Modified
Microcapsule Self-Healing System
for 4D Printing.
Front. Mater. 8:657777.
doi: 10.3389/fmats.2021.657777

Self-healing materials as a type of promising smart materials are gradually applied to electronics, biology, and engineering. In this study, we used *in situ* polymerization to make melamine-formaldehyde (MF) resin microcapsules to wrap the epoxy oxide as a repairing agent and Cu(MI)₄Br₂ as a latent-curing agent to protect epoxy oxide E-51 from broken melamine-formaldehyde resin microcapsules. In addition, graphene oxide was used as a reinforcing phase through its two-dimensional-layered structure to increase the tensile strength to 41.91 MPa, which is higher than the initial materials. The melamine-formaldehyde capsules and latent-curing agents were uniformly distributed in the materials according to the digital photos and scanning electron microscope (SEM) pictures. It is worth noting that the mechanical strength of the broken materials can be restored to 35.65 MPa after heating to 130°C for 2 h to repair the damage, and the self-healing efficiency reached up to 85.06%. Furthermore, we also fabricated the 4D printed material with a tensile strength of 50.93 MPa through a 3D printer. The obtained materials showed excellent repair effect, with a recovery rate of up to 87.22%. This study confirms that the designed self-healing system has potential applications in many areas due to its excellent self-healing performance, which provides valuable guidance for designing the 4D system.

Keywords: 4D printing, self-healing, microcapsules, polymermatrix composites, smart materials

INTRODUCTION

Smart materials have attracted widespread attention due to their shape and properties which can be altered with external environment changes, such as light, electricity, and magnetism (Wu et al., 2019). 3D printing smart materials, which are also referred to as “4D printing,” change configurations over time. So far, 4D printing has been used to develop many types of smart materials, such as shape-memory materials (Cheng et al., 2020), smart gel materials (Jang et al., 2020), and self-healing materials (Chen et al., 2016), which demonstrated great applications in the fields of biology (Aronsson et al., 2020; Kim et al., 2020), medicine (Javaid and Haleem, 2020; Lin et al., 2021), and bionics (Correa et al., 2020). Among them, the self-healing materials used for 3D printing mainly comprise soft active materials (SAMs), as a type of polymer, which can be mainly divided into five parts: engineering plastics (such as polyethersulfone, poly-ether-ether-ketone,

and polyphenylene sulfide), bioplastics (such as polylactic acid and polycaprolactone), thermoset materials, photosensitive resin, and polymer gels (Tan et al., 2020). The polymer should be selected and designed to achieve the properties required in accordance with the different environments and chemical properties. Wei et al. (2017) proposed 3D direct-write printing of ultraviolet (UV) cross-linking poly(lactic acid)-based inks, and its tensile strength reached 1.7 MPa. Shiblee et al. (2019) developed a shape memory hydrogel, which contains poly (N,N-dimethyl acrylamide-co-stearyl acrylate) [P(DMAAm-co-SA)], with the tensile strength of only 4.57 MPa. Although SAMs are characterized by high-tensile deformation and simple molding, their low-tensile strength limits their wide application (Enriquez-Cabrera et al., 2020). Therefore, some researchers are targeting hard materials.

Hard materials, which are aptly named, have generally high-tensile strengths. However, most hard materials cannot heal the physical damage autonomously, which is self-healing. The microcapsule strategy is one of the most prevalent self-healing strategies for hard materials, encapsulating substances that can produce healing effects without being affected by the curing of hard materials. When the microcapsules are broken, the coated core material flows out, and the corresponding chemical reaction occurs to achieve a self-healing effect. Zhao et al. (2020) prepared a microcapsule-type latent-curing agent with imidazole (IZ) as the core material, which is prepared by interfacial polymerization of triethanolamine (TEOA) and diphenylmethane diisocyanate (MDI). The tensile strength of IZ/E-51 reached 13.2 MPa. Nevertheless, the combination of microcapsules and graphene oxide (GO) has a wide range of applications in many areas in recent years, such as self-lubrication (Li H. et al., 2020; Li X. et al., 2020), thermal conductivity (Zhou Y. et al., 2020), and functionalization (Zhou Y. et al., 2020). Without doubts, GO itself has excellent properties, such as high specific surface areas, superb tensile strength, and electrical conductivity (Khan et al., 2020). On the one hand, recent studies on the combination of GO and microcapsules are mainly focused on the modification of GO to the microcapsules themselves. Ma et al. (2020) conceived a graphene-modified self-healing microcapsule, 1,6-diaminohexane as the inner core, and GO-isophorone diisocyanate (IPDI)-based prepolymer as the outer core. The results showed that the GO-modified microcapsules obtained a spherical shape with a mean diameter of 0.50 μm , and self-healing efficiency reaches 80.43%. A self-healing microcapsule material encapsulating linseed oil, using polyether ammonia molecules sutured with GO as the shell layer, was prepared by Li et al. (2019); the impedance modulus of the composite coating after healing was four orders of magnitude higher than that of pure polyurethane. On the other hand, some researchers have also incorporated GO into polymer substrates to prepare microcapsules self-healing systems with high-tensile strength. Akhan et al. (2020) developed UV-cured polyurethane GO nanocomposite microcapsules with a self-healing coating; the tensile strength of the self-healing coating came up to 36.10 MPa, which is the highest. As one of the hard materials, epoxy oxide has excellent mechanical properties and low shrinkage (less than 2%) (Farooq et al., 2020), so epoxy oxide remains virtually invariable

in volume after 4D printing and curing, with a slight increase in its original mechanical properties. For thermosetting hard resin, epoxy oxide requires the addition of curing agents to repair the damage (Gholipour-Mahmoudalilou et al., 2018; Gao et al., 2020; Seidi et al., 2020). The mechanical properties exhibit differently depending on the types of curing agents (Haddadi et al., 2019; Xie et al., 2020). The combination of epoxy oxide, microcapsules, graphene oxide, and 4D printing can be formed as a sort of self-healing material with high tensile strength and stable properties, showing a great potential for application in biology, medicine, and bionics.

In this study, we present a method to prepare the epoxy oxide-based self-healing system for 4D printing (**Scheme 1**). Microcapsules and $\text{Cu}(\text{MI})_4\text{Br}_2$ served as the healing units and latent-curing agents, respectively. Meanwhile, GO was also incorporated into the epoxy oxide self-healing system as the toughening phase to provide higher tensile strength. It is worth noting that the tensile strength of 4D printing GO that modified microcapsules of the epoxy oxide self-healing system can reach 50.93 MPa (the tensile strength of pouring samples with the same components is only 41.91 MPa), much higher than SAMs. When the scratches were healed, the tensile strength could still be restored to 44.42 MPa, with a high healing efficiency of up to 89.98%. The development of 4D printing epoxy oxide self-healing system will extend the usage of the new self-healing system and will be beneficial to a variety of practical 4D-printing-related applications, including material surface protection and aerospace structures.

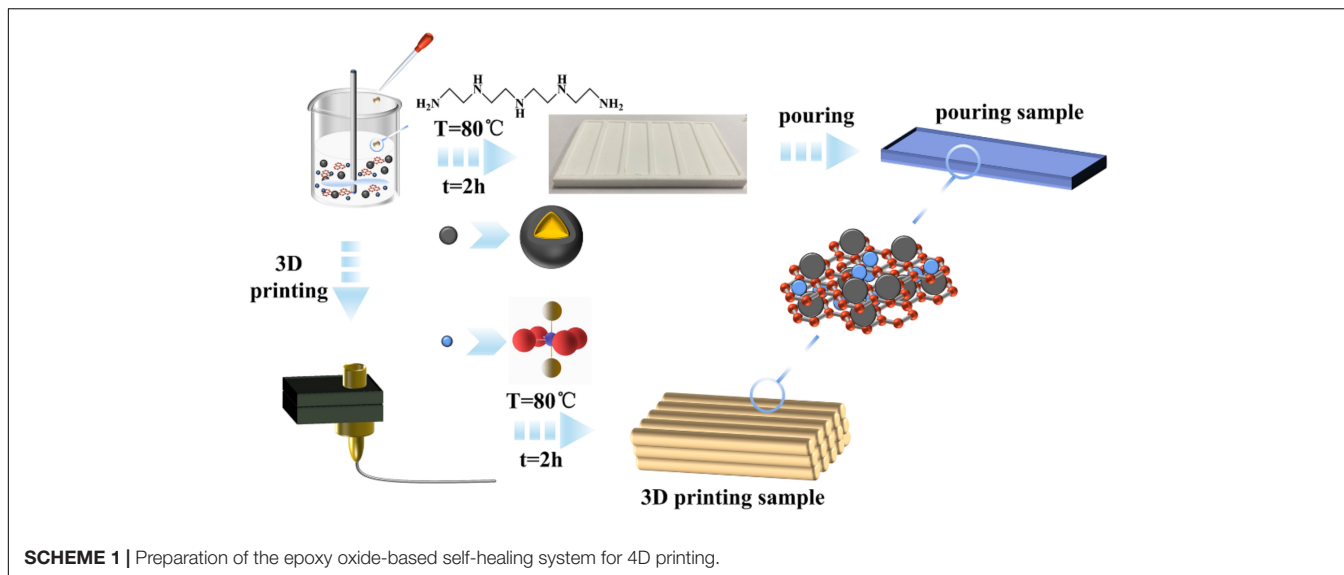
MATERIALS AND METHODS

Materials

Epoxy oxide (E-51), n-octanol, 2-methylimidazole (2-MI), and cupric bromide were supplied by Shanghai Macklin Biochemical Co., Ltd., China. Urea, melamine, tetraethylenepentamine (TEPA), and sodium dodecylbenzenesulfonate (SDBS) were obtained from Tianjin Guangfu Fine Chemical Research Institute, China. Formaldehyde was made by Liaoning Quan Rui Reagent Co., Ltd., China.

Preparation of Epoxy Oxide Microcapsules

The microcapsules, with phenolic resin as the wall and epoxy oxide as the core, were prepared *via* an *in situ* polymerization microencapsulation process. The fabrication method consisted of three steps, which can be described as the following: First, melamine (3.2 g), urea (0.8 g), and formaldehyde solution (2.7 g) were mixed in a 100 mL beaker equipped with a magnetic stirrer. The pH value of the solution was adjusted to 8–9 by slowly adding TEOA solution and continuing reaction for 1 h under 70°C. Second, a certain amount of epoxy oxide E-51 was added to 100 mL of 1 wt% aqueous solution of SDBS with the above phenolic resin at 25°C. The mixture was stirred at 700 rpm for 10 min to form an emulsion. Third, the pH of the reaction mixture was slowly tuned to 3–4 by adding 0.1 mol/L hydrochloric acid. The resultant microcapsules were filtrated and



washed with acetone, ethanol, and deionized water several times to remove impurities. The synthesis reaction equation is shown in **Supplementary Schemes 1–3**.

Preparation of the Latent-Curing Agent

CuBr_2 (11.17 g, 0.05 mol) and 2-MI (16.42 g, 0.2 mol) were dissolved in the beaker with methanol solution (50 mL) by ultrasonication. Then, the two solutions were mixed and stirred at 25°C for 24 h. The sediment was obtained by centrifugation and dried at 50°C in a vacuum oven for 6 h.

Preparation of the 3D Printing Sample

About 0.3 wt% (based on the E-51 epoxy oxide) GO was added to 10 g epoxy oxide and stirred magnetically for 30 min at 800 rpm, and sonicated for 30 min, and then, 1 g of microcapsules and 0.2 g of the latent-curing agent were added sequentially and stirred magnetically at 400 rpm for 5 min; at the same time, 0.15 g of TEPA was added through the whole process and additionally stirred magnetically for 2 min. All of the above steps were carried out at 25°C. The mixture was degassed by vacuum to remove the air mixed into the mixture during the mixing process. The degassed mixture was then added to the resin bath of the 3D printer (Nordson ASYMTEK CN DS Quantum Q-6800, American). A STL file of the structure, which we designed, was loaded into Fluidmove software in order to generate a series of G.codes. The thickness of the single print layer was set to 500 μm . The 3D printer then read the G.code and printed layer by layer at the printing speed of 1 mm/s by using the syringe print head in a predetermined path. The whole process was carried out at 60°C. The finished product was removed from the substrate and cured at 80°C for 2 h.

Preparation of Pouring Sample

About 0.3 wt% (based on the E-51 epoxy oxide) GO was added to 10 g epoxy oxide and stirred magnetically for 30 min at 800 rpm, and sonicated for 30 min, and then, 1 g of microcapsules and 0.2 g

of the latent-curing agent were added sequentially and stirred magnetically at 400 rpm for 5 min; at the same time, 0.15 g TEPA was added through the whole process and additionally stirred magnetically for 2 min. All of the above steps were carried out at 25°C. The mixture was poured in a preheated Teflon mold, which was preheated at 100°C, vacuumed to remove air bubbles, and heated at 80°C for 2 h. The samples were allowed to cool at 25°C and were then removed.

Preparation of Self-Healing Samples

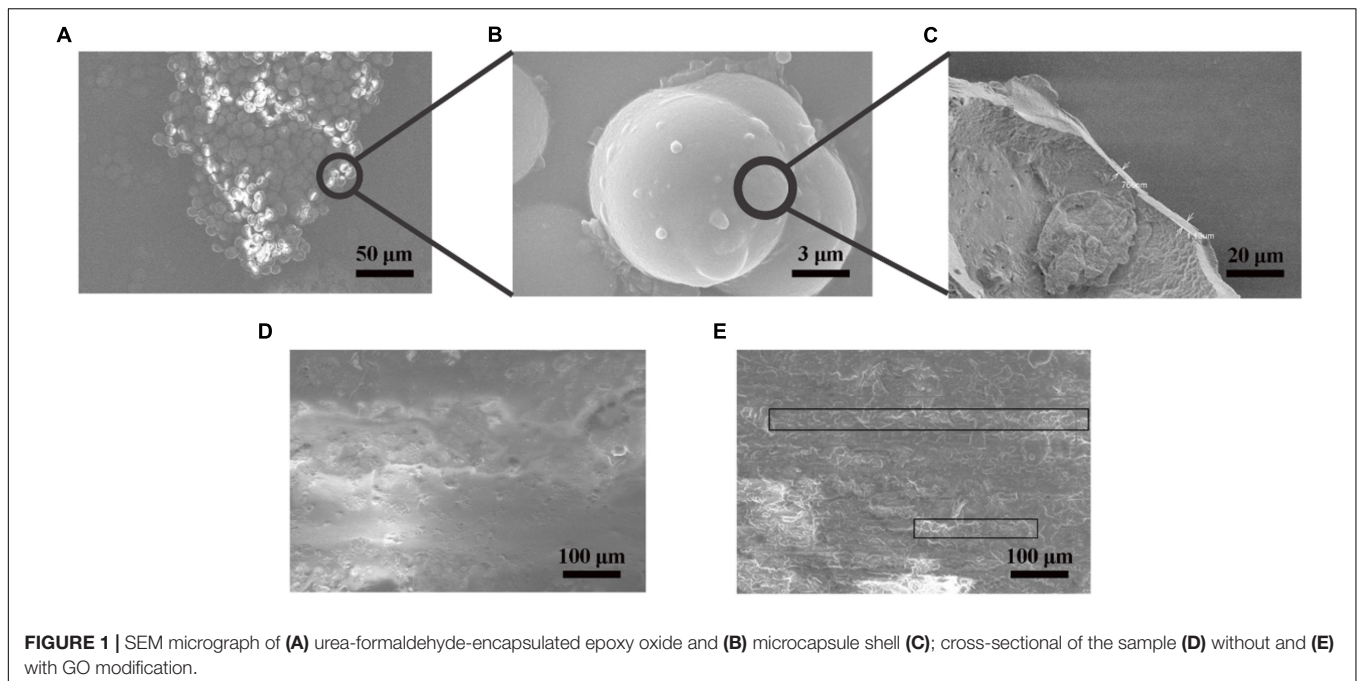
The surface of samples was cut a scratch with a depth of 1 mm, with an scalpel. Then, the scratch samples were immediately heated at 130°C for 2 h. The self-healing process of the sample was recorded by taking photographs. Healing performance was confirmed by comparing the tensile strength of original, scratch, and scratch repair samples.

Characterization

Micrographs of the microcapsules were taken with Field Emission Scanning Electron Microscope (FE-SEM) (Hitachi, Regulus 8220, Japan) at 5 kV and a current of 10 μA . FTIR studies were conducted on a Bruker spectrophotometer (ALPHA, German). The powdered samples of 2-MI and $\text{Cu}(\text{MI})_4\text{Br}_2$ were mixed with KBr at a ratio of 1:100 to produce tablets for FTIR measurement. The thermogravimetric analysis of 2-MI, $\text{Cu}(\text{MI})_4\text{Br}_2$, and microcapsules were conducted by Mettler Toledo TGA 2 (Switzerland) at air atmosphere with the heating interval ranging from 25 to 800°C and at the speed of 5°C/min. The tensile strength of pouring samples and 3D printing samples were tested by Instron 3400 (United States), and the tensile state was 2 mm/min under 5 kN load.

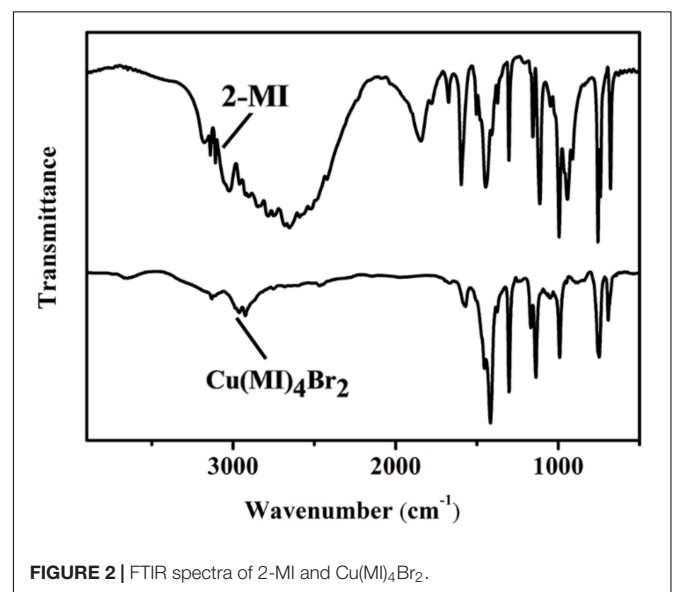
RESULTS AND DISCUSSION

The capsules present a regular spherical configuration, and their size was uniform, which prove the correctness of the



colloid theory (Figures 1A,B). The diameters of microcapsule are about 10–12 μm , and their surface is smooth, which is caused by precipitation, aggregation, and deposition of polyuria; microcapsules with rough shell morphology have also been reported (Keller et al., 2007). Due to the brittle nature of microencapsulated shells, after the microcapsules were ruptured by compression force, a clear image of a core-shell structure of microcapsule can be observed under SEM (Figure 1C). It can be clearly seen to have a width of 0.7–1.5 μm , proving that the microcapsules are the core-shell structure rather than a mixture state. The cross-section of the self-healing system without GO is smooth and appears to have no obvious structure (Figure 1D). When the self-healing system was modified with graphene oxide, its cross-section shows clearly that GO sheets were formed with a tightly layered structure, comprising waves that look like fine alternating layers (Figure 1E). The reason is that the reactive groups achieve robust interaction with epoxy oxide through covalent or hydrogen bonding, which greatly improves the interfacial compatibility of the GO with the epoxy oxide matrix (Yu et al., 2019). The structure of the self-healing system changes from disorder to layer, with the addition of graphene oxide, which will improve its toughness to a great extent (Ye et al., 2014).

2-methylimidazole can react with copper ions to form stable metal complexes with square pyramidal geometry, namely, $\text{Cu}(\text{MI})_4\text{Br}_2$ (Zhu et al., 2015). Br^- occupies two vertices, and MI groups are distributed at the four vertices in the middle of the diamond. Improving the temperature will lead to the dissociation of $\text{Cu}(\text{MI})_4\text{Br}_2$ and the release of MI groups, which will react with epoxy oxide to change the repair effect (Supplementary Scheme 4; Pilawka and Maka, 2011; Tripathi et al., 2015). The FTIR spectra of 2-MI and $\text{Cu}(\text{MI})_4\text{Br}_2$ are illustrated in Figure 2. All of the characteristic bands of the MI group can be clearly

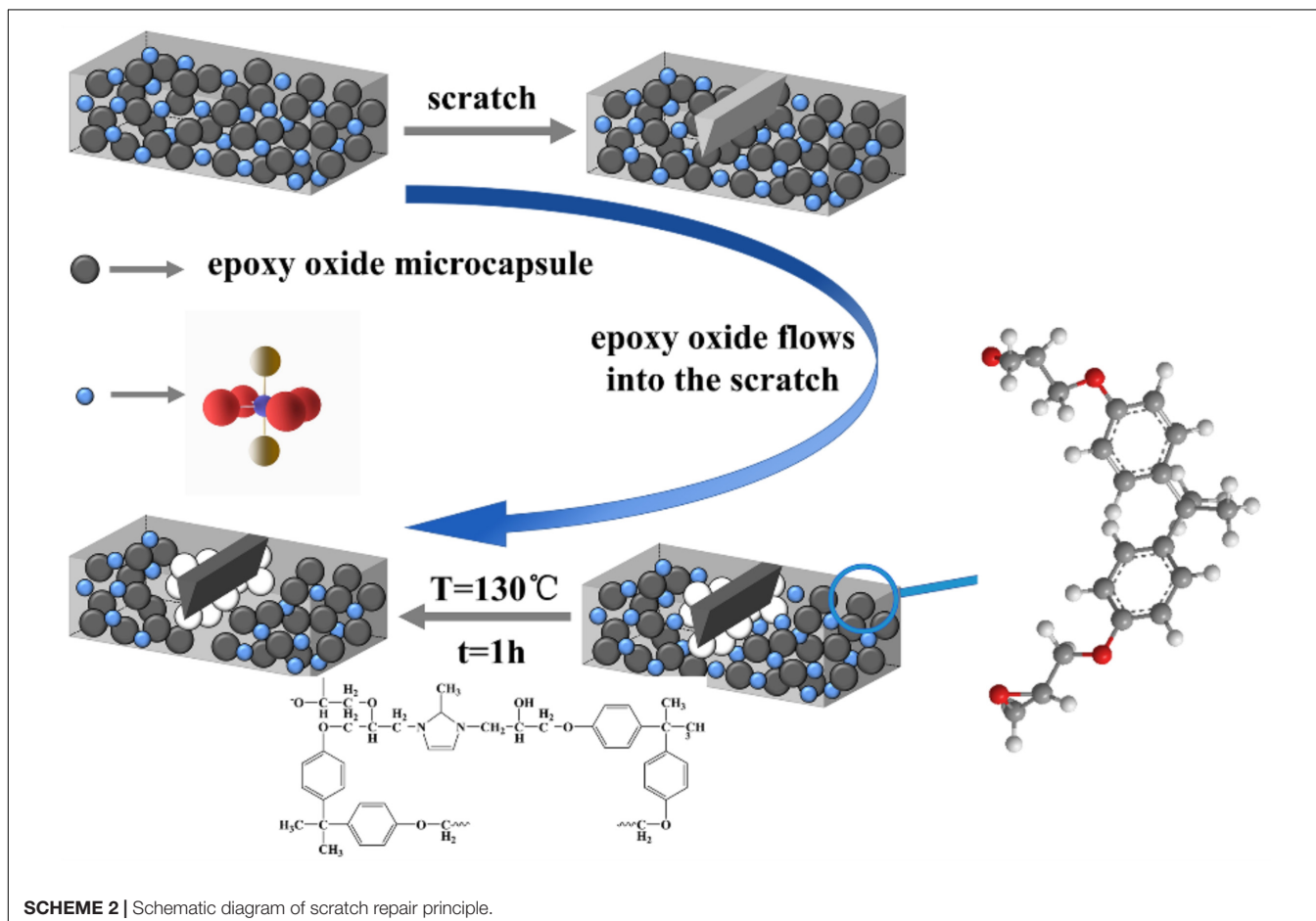
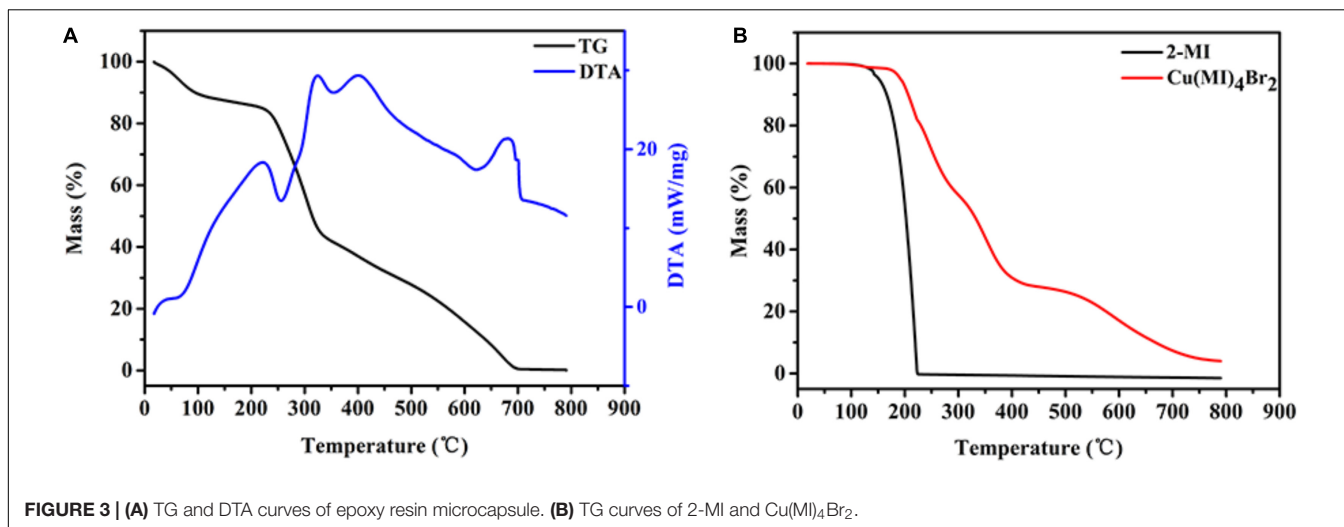


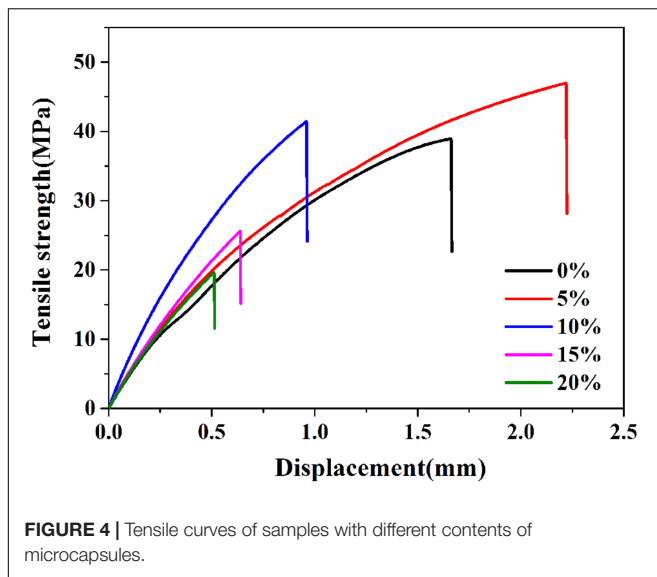
observed, including N–H stretching at $3,400\text{ cm}^{-1}$, N–H wagging vibration at 650 cm^{-1} , C–N stretching at $1,600\text{ cm}^{-1}$, C = N stretching at $1,700\text{ cm}^{-1}$, = CH rocking vibration at $1,460\text{ cm}^{-1}$. But, in the FTIR of $\text{Cu}(\text{MI})_4\text{Br}_2$, the N–H stretching cannot be observed. That is because the H on the nitrogen atom of 2-MI secondary amine reacts with Cu ions. The appearance of these peaks shows that $\text{Cu}(\text{MI})_4\text{Br}_2$ was successfully prepared.

Figure 3A illustrates the TG and DTA curves of epoxy oxide microcapsule. The evaporation of water is mainly below 113°C . When the temperature reached 316°C , the wall of microcapsule decomposed. The core material began to evaporate in large

quantities due to the loss of protection of the wall under high temperature. **Figure 3B** shows the TG curves of 2-MI and $\text{Cu}(\text{MI})_4\text{Br}_2$. 2-MI begins to decompose at 152°C , while the decomposition temperature of $\text{Cu}(\text{MI})_4\text{Br}_2$ is 216°C , suggesting the improved thermal stability of MI groups after forming a complex. The schematic diagram of the self-healing system

is shown in **Scheme 2**. The microcapsules and the latent-curing agent $\text{Cu}(\text{MI})_4\text{Br}_2$ are evenly embedded in the epoxy oxide substrate. Under the action of external destruction, the microcapsules will break, leading to the flow out of epoxy oxide. In addition, the $\text{Cu}(\text{MI})_4\text{Br}_2$ will be decomposed at high temperature in the MI group, which will solidify the epoxy





oxide at the damaged area to achieve the purpose of repair. Therefore, the core-shell structure also ensures the integrity of the epoxy oxide inwardly under high temperature, which will not be thermally decomposed and react with the MI groups cured by the high-temperature decomposition of the latent-curing agent $\text{Cu}(\text{MI})_4\text{Br}_2$. Meanwhile, the stabilized complex structure of $\text{Cu}(\text{MI})_4\text{Br}_2$ ensures that the MI groups will not react with the epoxy oxide matrix when heating at 100°C but will decompose out of the complexed structure when it reaches 130°C and then react with the epoxy oxide overflow from microcapsules for curing.

Figure 4 shows the effect of different contents of microcapsules on the mechanical properties of the system. With the increasing number of microcapsules embedded, the tensile strength of the sample first shows an increasing trend and then a decreasing trend. Microcapsules in epoxy oxide can be seen as “enlarged” vacancy defects, and epoxy oxide substrate surface area can be enlarged. When the fracture crack extends to the location where the microcapsules are in contact with the epoxy oxide, there is an interface problem between shell materials of microcapsules and epoxy oxide matrix because both materials are different (Yuan et al., 2019). The walls of the microcapsules allow the stress to be dispersed rather than following a straight line. The distance between microcapsules reached the optimum distance when 10% content of microcapsules was added to the epoxy oxide matrix. While the sample is stretched, the distance of atoms, molecules, and other components at the fracture increases, the repulsive force decreases, and tension occurs macroscopically; a greater tensile stress is needed to make the sample fracture because the microcapsules disperse the stress and reduce the strain, which makes the final manifestation of large stress and a small strain, resulting in a large Young’s modulus. When the content of microcapsules is 5%, the distance between microcapsules increases so that few parts of the tensile stress will extend between the walls of microcapsules and epoxy oxide, augmenting its tensile strength. When the content of

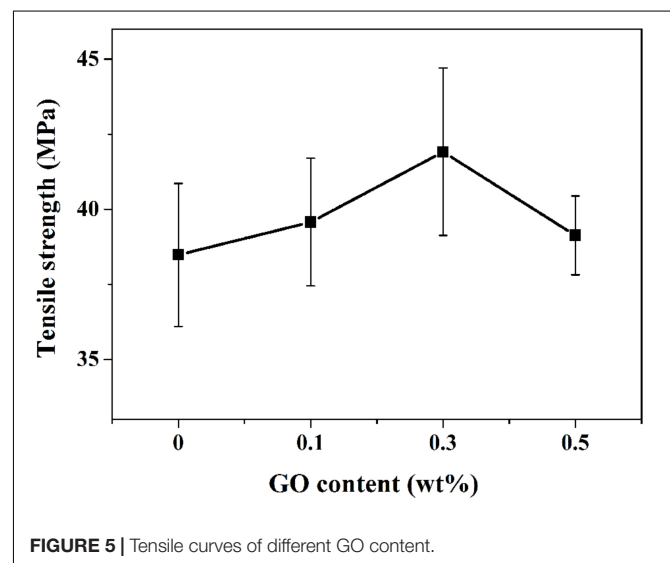
TABLE 1 | Four kinds of samples with different compositions.

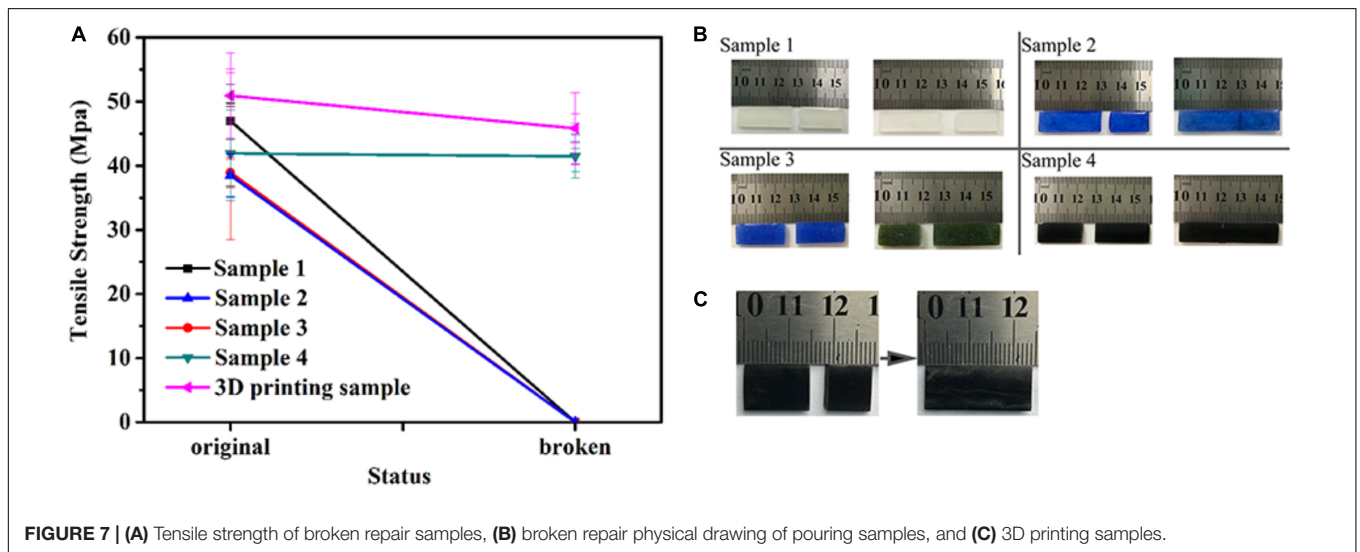
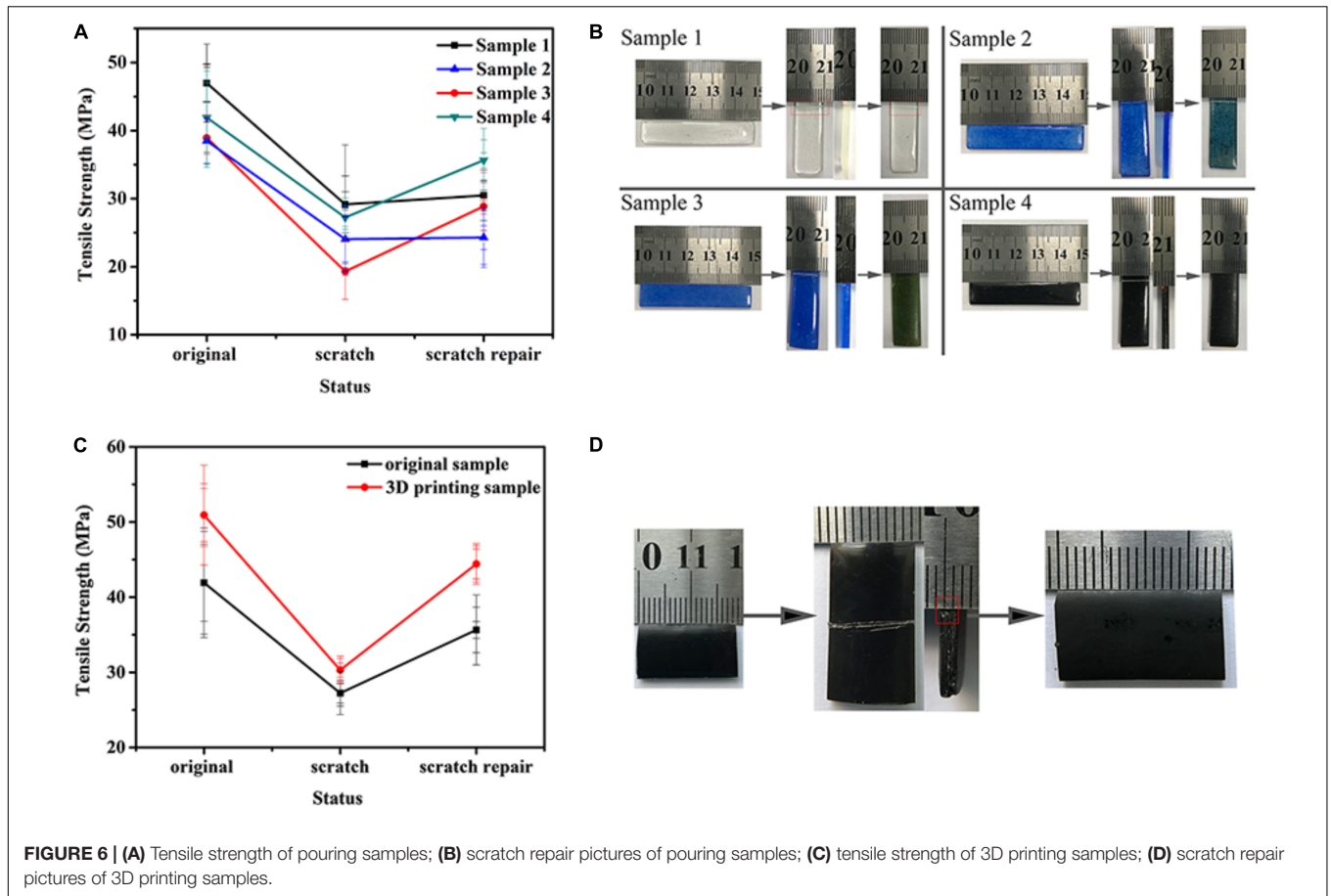
	$\text{Cu}(\text{MI})_4\text{Br}_2$	Microcapsule	Graphene oxide
Sample 1	×	×	×
Sample 2	✓	×	×
Sample 3	✓	✓	×
Sample 4	✓	✓	✓

microcapsules increased to 15 and 20%, the distance between microcapsules decreased, but the existence of microcapsules greatly reduces the continuity of epoxy oxide substrate, the macroscopic tensile strength decreases sharply, and the microscopic displacement of atoms and molecules is greatly restricted, so that the elastic deformation decreases sharply and fracture occurs at small displacement, which results in the decrease of its tensile strength. In order to make the sample possess optimum tensile strength and repair efficiency, we chose the blending amount of microcapsule to be 10 wt%.

The effect of GO on the tensile strength of the sample, which contains microcapsules and $\text{Cu}(\text{MI})_4\text{Br}_2$, is carefully investigated as shown in **Figure 5**. Test results showed that the tensile strength of the samples increases significantly with increasing GO content. The enhancement of GO to the tensile strength of the sample is mainly due to the chemical bonding between GO and $\text{Cu}(\text{MI})_4\text{Br}_2$ /microcapsule/epoxy oxide segments in the GO-modified microcapsule self-healing system. The strong interfacial covalent bonding is favorable to the loading transfer from the polymer matrix to GO, with superior tensile strength (Xia et al., 2015). Furthermore, because of the immense modulus difference between GO and epoxy oxide, GO functions as a stress-concentration point and induces microcracks around it, which consumes additional fracture energy to improve the tensile strength (Chen et al., 2017).

Several experiments have been conducted to analyze the effect of each component on the overall performance. **Table 1**





shows four kinds of samples with different compositions. Their corresponding repair experiment and tensile strength are shown in **Figure 6**. According to **Figure 6A**, samples without added microcapsules cannot achieve a self-healing effect. It indicates that microcapsules are the necessary healing units in the self-healing system. While the microcapsules were incorporated

into the epoxy oxide matrix (sample 3), the tensile strength increased to 0.45 MPa compared with that of sample 2, demonstrating that a small portion of the stress was dispersed, along with the shells of the microcapsules and the epoxy oxide matrix, resulting in an increase in the tensile strength. The tensile strength of GO-modified samples (sample 4) can restore

to 85.04%, while the sample 3 without GO-modified samples only restores to 63.07%. This demonstrates that GO as a toughening phase can improve to some extent the reduction of the tensile strength of the samples due to the lower continuity of the epoxy oxide matrix, which is caused by the incorporation of microcapsules and latent-curing agents $\text{Cu}(\text{MI})_4\text{Br}_2$. The stress diffused in the network structure, which was composed of GO and epoxy oxide matrix, which required higher stress to fracture the sample, and the tensile stress increased. The tensile strength curves and the scratch repair pictures of 3D printing samples are shown in **Figures 6C,D**. After 3D printing, the tensile strength of the sample is 21.51% higher than the pouring sample 4. After repair, the tensile strength of 3D printing sample can be restored to 87.23%, which is higher than that of the pouring sample at 85.04%. Because the potential difference inside the epoxy oxide is smaller than the gravitational force between the microcapsules, the little number of microcapsules coalesces and sinks. Nevertheless, the 3D printed samples were printed directly layer by layer, with a thickness of 500 μm , and cured by heating while printing. This minimized the settling of the microcapsules, and the dispersion of each component in the epoxy oxide was higher in the 3D printed samples compared with the pouring samples, which showed the macroscopic improvement of tensile strength.

At the same time, we also text the extreme situation of the sample. The tensile strength of the broken and repair of samples are given in **Figure 7**. The pouring samples 1, 2, and 3 cannot repair the broken, but sample 4 and 3D printing sample can repair the broken. After repair, the tensile strength of sample 4 can be recovered to 98.90%, and the tensile strength of 3D printing sample can be recovered to 89.97%. Unlike scratch repair, the broken repair efficiency of Sample 4 was higher than 3D-printed samples. It can be explained that, because the internal potential difference of epoxy oxide is less than the gravitational force between microcapsules, a small number of microcapsules coalesce and sink, which makes the dispersion of microcapsules uneven and epoxy oxide flow from the broken microcapsules to gather in these sinking parts. The repair efficiency of the pouring sample was increased to 98.90% because the two sections of the fracture overlapped together at both ends under the external force, while the epoxy oxide overflowing from the aggregated microcapsules deposited at the bottom of the sample was squeezed and spread in all directions, causing the non-uniformity of the repair (the repair efficiency of the upper part of the sample was lower than that of the lower part). The 3D-printed sample had the maximum repair efficiency of 89.97% because the repair area was only around the broken microcapsules due to a less settling phenomenon.

CONCLUSION

In summary, we report an approach to develop a GO-modified microcapsule self-healing system for 4D printing.

The measurement of SEM showed that the epoxy oxide microcapsules, as the healing unit, have a smooth surface, uniform particle size at 10–12 μm , and 0.70–1.5 μm microcapsule shell thickness. The thermodynamic measurement indicated that the thermal decomposition temperature of the prepared microcapsule is 316°C, which can largely protect the epoxy oxide inside the microcapsules from decomposition under high temperature. The tensile measurement has shown that the tensile strength of the 3D printing sample modified by GO was 21.51% more than the pouring sample, reaching to 50.93 MPa. Physical restoration experiments have proved that scratch repair efficiency comes up to 87.23% and broken repair efficiency carries to 89.97%. The incorporation of 10 wt% microcapsules can improve the tensile strength of the samples, which is attributed to the dispersion of stress between the microcapsule shell and the epoxy oxide matrix. The incorporation of a 0.3 wt% (based on epoxy oxide) GO further increased the mechanical strength of the sample, which is facilitated by chemical bonding between GO and $\text{Cu}(\text{MI})_4\text{Br}_2$ /microcapsule/epoxy oxide segments and the immense modulus difference between GO and epoxy oxide. This GO-modified microcapsule self-healing system holds great potential in the field of engineering, surface protection, and electronic packaging.

DATA AVAILABILITY STATEMENT

The original contributions presented in the study are included in the article/**Supplementary Material**, further inquiries can be directed to the corresponding author/s.

AUTHOR CONTRIBUTIONS

BM performed the main experimental work and characterization. YZ helped with tensile strength testing. YW and ML assisted with relevant experiments and characterization. DL conducted instructional work for this experiment. All authors contributed to the article and approved the submitted version.

FUNDING

This work was supported by the National Natural Science Foundation of China (Nos. 51627805 and U19A2085), the Optical Valley Science Research Project, WEHDZ (No. 2019001).

SUPPLEMENTARY MATERIAL

The Supplementary Material for this article can be found online at: <https://www.frontiersin.org/articles/10.3389/fmats.2021.657777/full#supplementary-material>

REFERENCES

- Akhan, S., Oktay, B., Özdemir, O. K., Madakbaş, S., and Kayaman Apohan, N. (2020). Polyurethane graphene nanocomposites with self-healing properties by azide-alkyne click reaction. *Mater. Chem. Phys.* 254:123315. doi: 10.1016/j.matchemphys.2020.123315
- Aronsson, C., Jury, M., Naeimipour, S., Boroojeni, F. R., Christofferson, J., Lifwergren, P., et al. (2020). Dynamic peptide-folding mediated biofunctionalization and modulation of hydrogels for 4D bioprinting. *Biofabrication* 12:035031. doi: 10.1088/1758-5090/ab9490
- Chen, B., Tang, J., Zhang, G., Chen, S., and Zhang, J. (2017). Properties and morphologies of epoxy resin based composites reinforced by polyurethane and graphene Oxide. *Mater. Trans.* 58, 842–844. doi: 10.2320/matertrans.M2016464
- Chen, L., Li, W., Liu, Y., and Leng, J. (2016). Nanocomposites of epoxy-based shape memory polymer and thermally reduced graphite oxide: mechanical, thermal and shape memory characterizations. *Compos. Part B Eng.* 91, 75–82. doi: 10.1016/j.compositesb.2016.01.019
- Cheng, C.-Y., Xie, H., Xu, Z.-Y., Li, L., Jiang, M.-N., Tang, L., et al. (2020). 4D printing of shape memory aliphatic copolyester via UV-assisted FDM strategy for medical protective devices. *Chem. Eng. J.* 396:125242. doi: 10.1016/j.cej.2020.125242
- Correa, D., Poppinga, S., Mylo, M. D., Westermeier, A. S., Bruchmann, B., Menges, A., et al. (2020). 4D pine scale: biomimetic 4D printed autonomous scale and flap structures capable of multi-phase movement. *Philos. Trans. A Math. Phys. Eng. Sci.* 378:20190445. doi: 10.1098/rsta.2019.0445
- Enriquez-Cabrera, A., Rapakousiou, A., Piedrahita Bello, M., Molnár, G., Salmon, L., and Bousseksou, A. (2020). Spin crossover polymer composites, polymers and related soft materials. *Coord. Chem. Rev.* 419:213396. doi: 10.1016/j.ccr.2020.213396
- Farooq, U., Teuwen, J., and Dransfeld, C. (2020). Toughening of epoxy systems with interpenetrating polymer network (IPN): a review. *Polymers* 12:1908. doi: 10.3390/polym12091908
- Gao, X., Yan, R., Lv, Y., Ma, H., and Ma, H. (2020). In situ pretreatment and self-healing smart anti-corrosion coating prepared through eco-friendly water-base epoxy resin combined with non-toxic chelating agents decorated biomass porous carbon. *J. Clean. Prod.* 266:121920. doi: 10.1016/j.jclepro.2020.121920
- Gholipour-Mahmoudalilou, M., Roghani-Mamaqani, H., Azimi, R., and Abdollahi, A. (2018). Preparation of hyperbranched poly (amidoamine)-grafted graphene nanolayers as a composite and curing agent for epoxy resin. *Appl. Surface Sci.* 428, 1061–1069. doi: 10.1016/j.apsusc.2017.09.237
- Haddadi, S. A., Ramazani, S. A. A., Mahdavian, M., Taheri, P., Mol, J. M. C., and Gonzalez-Garcia, Y. (2019). Self-healing epoxy nanocomposite coatings based on dual-encapsulation of nano-carbon hollow spheres with film-forming resin and curing agent. *Compos. Part B Eng.* 175:107087. doi: 10.1016/j.compositesb.2019.107087
- Jang, J. W., Park, J. H., Kim, I. J., Sim, J. H., Yu, S. G., Lee, D. J., et al. (2020). Preparation and characterization of thermoresponsive poly(N-isopropylacrylamide-co-N-isopropylmethacrylamide) hydrogel materials for smart windows. *J. Appl. Polym. Sci.* 138:49788. doi: 10.1002/app.49788
- Javadi, M., and Haleem, A. (2020). Significant advancements of 4D printing in the field of orthopaedics. *J. Clin. Orthop. Trauma* 11(Suppl. 4), S485–S490. doi: 10.1016/j.jcot.2020.04.021
- Keller, M. W., White, S. R., and Sottos, N. R. (2007). A self-healing poly(Dimethyl Siloxane) elastomer. *Adv. Funct. Mater.* 17, 2399–2404. doi: 10.1002/adfm.200700086
- Khan, F., Khan, M. S., Kamal, S., Arshad, M., Ahmad, S. I., and Nami, S. A. A. (2020). Recent advances in graphene oxide and reduced graphene oxide based nanocomposites for the photodegradation of dyes. *J. Mater. Chem. C* 8, 15940–15955. doi: 10.1039/d0tc03684f
- Kim, S. H., Seo, Y. B., Yeon, Y. K., Lee, Y. J., Park, H. S., Sultan, M. T., et al. (2020). 4D-bioprinted silk hydrogels for tissue engineering. *Biomaterials* 260:120281. doi: 10.1016/j.biomaterials.2020.120281
- Li, H., Chen, S., Li, Z., Feng, Y., and Zhang, M. (2020). Preparation of PU/GO hybrid wall microcapsules and their self-lubricating properties for epoxy composites. *Colloids Surf. A Physicochem. Eng. Asp.* 596:124729. doi: 10.1016/j.colsurfa.2020.124729
- Li, J., Li, Z., Feng, Q., Qiu, H., Yang, G., Zheng, S., et al. (2019). Encapsulation of linseed oil in graphene oxide shells for preparation of self-healing composite coatings. *Prog. Org. Coat.* 129, 285–291. doi: 10.1016/j.porgcoat.2019.01.024
- Li, X., Yu, R., He, Y., Zhang, Y., Yang, X., Zhao, X., et al. (2020). Four-dimensional printing of shape memory polyurethanes with high strength and recyclability based on Diels-Alder chemistry. *Polymer* 200:122532. doi: 10.1016/j.polymer.2020.122532
- Lin, C., Liu, L., Liu, Y., and Leng, J. (2021). 4D printing of bioinspired absorbable left atrial appendage occluders: a proof-of-concept study. *ACS Appl. Mater. Interfaces* 13, 12668–12678. doi: 10.1021/acsmi.0c17192
- Ma, Y., Zhang, Y., Liu, J., Ge, Y., Yan, X., Sun, Y., et al. (2020). GO-modified double-walled polyurea microcapsules/epoxy composites for marine anticorrosive self-healing coating. *Mater. Des.* 189:108547. doi: 10.1016/j.matdes.2020.108547
- Pilawka, R., and Maka, H. (2011). Epoxy adhesive formulations using latent imidazole metal cation complexes. *Pol. J. Chem. Technol.* 13, 63–66.
- Seidi, F., Jouyandeh, M., Taghizadeh, M., Taghizadeh, A., Vahabi, H., Habibzadeh, S., et al. (2020). Metal-organic framework (MOF)/Epoxy coatings: a review. *Materials* 13:2881. doi: 10.3390/ma13122881
- Shiblee, M. D. N. I., Ahmed, K., Kawakami, M., and Furukawa, H. (2019). 4D printing of shape-memory hydrogels for soft-robotic functions. *Adv. Mater. Technol.* 4:1900071. doi: 10.1002/admt.201900071
- Tan, L. J., Zhu, W., and Zhou, K. (2020). Recent progress on polymer materials for additive manufacturing. *Adv. Funct. Mater.* 30:2003062. doi: 10.1002/adfm.202003062
- Tripathi, M., Dwivedi, R., Kumar, D., and Roy, P. K. (2015). Thermal activation of mendable epoxy through inclusion of microcapsules and imidazole complexes. *Polym. Plast. Technol. Eng.* 55, 129–137. doi: 10.1080/03602559.2015.1070866
- Wei, H., Zhang, Q., Yao, Y., Liu, L., Liu, Y., and Leng, J. (2017). Direct-write fabrication of 4D active shape-changing structures based on a shape memory polymer and its nanocomposite. *ACS Appl. Mater. Interfaces* 9, 876–883. doi: 10.1021/acsmi.6b12824
- Wu, H., Chen, P., Yan, C., Cai, C., and Shi, Y. (2019). Four-dimensional printing of a novel acrylate-based shape memory polymer using digital light processing. *Mater. Des.* 171:107704. doi: 10.1016/j.matdes.2019.10.7704
- Xia, S., Liu, Y., Pei, F., Zhang, L., Gao, Q., Zou, W., et al. (2015). Identical steady tribological performance of graphene-oxide-strengthened polyurethane/epoxy interpenetrating polymer networks derived from graphene nanosheet. *Polymer* 64, 62–68. doi: 10.1016/j.polymer.2015.03.036
- Xie, W., Huang, S., Tang, D., Liu, S., and Zhao, J. (2020). Synthesis of a furfural-based DOPO-containing co-curing agent for fire-safe epoxy resins. *RSC Adv.* 10, 1956–1965. doi: 10.1039/c9ra06425g
- Ye, X. J., Song, Y. X., Zhu, Y., Yang, G. C., Rong, M. Z., and Zhang, M. Q. (2014). Self-healing epoxy with ultrafast and heat-resistant healing system processable at elevated temperature. *Compos. Sci. Technol.* 104, 40–46. doi: 10.1016/j.compscitech.2014.08.028
- Yu, Z., Wang, Z., Li, H., Teng, J., and Xu, L. (2019). Shape memory epoxy polymer (SMEP) composite mechanical properties enhanced by introducing graphene oxide (GO) into the matrix. *Materials* 12:1107. doi: 10.3390/ma12071107
- Yuan, L., Sun, T., Hu, H., Yuan, S., Yang, Y., Wang, R., et al. (2019). Preparation and characterization of microencapsulated ethylenediamine with epoxy resin for self-healing composites. *Sci. Rep.* 9:18834. doi: 10.1038/s41598-019-55268-7
- Zhao, L., Yang, X., Ma, L., and Li, Q. (2020). Preparation of imidazole embedded polyurea microcapsule for latent curing agent. *J. Appl. Polym. Sci.* 137:49340. doi: 10.1002/app.49340
- Zhou, J., Zhao, J., Li, H., Cui, Y., and Li, X. (2020). Enhanced thermal properties for nanoencapsulated phase change materials with functionalized graphene oxide

- (FGO) modified PMMA. *Nanotechnology* 31:295704. doi: 10.1088/1361-6528/ab898b
- Zhou, Y., Li, C., Wu, H., and Guo, S. (2020). Construction of hybrid graphene oxide/graphene nanoplates shell in paraffin microencapsulated phase change materials to improve thermal conductivity for thermal energy storage. *Colloids Surfaces A Physicochem. Eng. Asp.* 597:124780. doi: 10.1016/j.colsurfa.2020.124780
- Zhu, D. Y., Rong, M. Z., and Zhang, M. Q. (2015). Self-healing polymeric materials based on microencapsulated healing agents: from design to preparation. *Prog. Polym. Sci.* 4, 175–220. doi: 10.1016/j.progpolymsci.2015.07.002

Conflict of Interest: The authors declare that the research was conducted in the absence of any commercial or financial relationships that could be construed as a potential conflict of interest.

Copyright © 2021 Ma, Zhang, Wei, Li and Li. This is an open-access article distributed under the terms of the Creative Commons Attribution License (CC BY). The use, distribution or reproduction in other forums is permitted, provided the original author(s) and the copyright owner(s) are credited and that the original publication in this journal is cited, in accordance with accepted academic practice. No use, distribution or reproduction is permitted which does not comply with these terms.